J. Cent. South Univ. (2017) 24: 957−966
DOI: 10.1007/s11771-017-3498-5

Springer

Collapse analysis of tunnel floor in karst area based on Hoek-Brown rock media

YANG Xiao-li(杨小礼), LI Zheng-wei(李正伟), LIU Zheng-an(刘拯安), XIAO Hai-bo(肖海波)

School of Civil Engineering, Central South University, Changsha 410075, China

Abstract: Collapse shape of tunnel floor in Hoek-Brown rock media is investigated with the functional catastrophe theory. The stability of rock system in tunnel floor, which is determined by thickness, half collapse width, half length of cave and detaching curve, has great secure and economic significance in practical engineering. To investigate the failure mechanisms and the outline of detaching block, a reliable damage model is presumed by making reference to the limit analysis theory. The analytical solutions of detaching curve, half collapse width on tunnel floor and the critical and maximum values of collapse thickness are derived based on Hoek-Brown criterion and functional catastrophe theory. The result shows that 0.5 is a most probable condition for instability, and the shape of detaching curve is a part of parabola. It is reasonable by comparing with previous theory and analogous experiments. The effects of major factors on thickness and half collapse width are further discussed. Numerical calculations and parametric analysis are carried out to illustrate the effects of different parameters on the mechanism, which is significant to the stability analysis of tunnel floor in rock media.

Key words: karst; functional catastrophe theory; Hoek-Brown criterion; safety thickness; tunnel floor; upper bound

1 Introduction

The stability analysis of tunnel floor is an important topic, and has been investigated by several scholars. The development and utilization of underground space, including metros, underwater tunnels, underground caverns and mines, have led to a further study of geotechnical engineering. There are many new leading sciences derived from practical engineering along with the in-depth research. Although there have been many theoretical and practical explorations, underground engineering always suffers from a lot of problems. In fact, numerous damages caused by rockburst, water inrush and karst have been a serious problem to the quality of construction and the safety of people. The frequency and the level of rock stratum instability, including tunnel roof or floor collapse and water inrush have showed a growing tendency.

The strength envelops are nonlinear in the normal and shear stress space. The instability of rock system has been investigated by many scholars, while it still remains an hard issue in theoretical study and engineering practice due to the characteristics of sudden and complexity. The embryonic stage of sudden instability study is quasi-static, therefore the strength theory is adopted by scholars to analyze the stability and safety thickness of rock system. Actually, the occurrence of collapse or instability is dynamic, and the entire process will release a great deal of elastic energy gathered in the rock system. It is a kind of complex behavior under highly nonlinear state.

In general, on the basis of results obtained by GUGLIELMETTI et al [1], the collapse of tunnel can be categorized in terms of factors as follows: daylight collapse, underground collapse, rock burst, inrush of water, and portal collapse. The methods and theories employed in all kinds of issues are diverse. The traditional way to ensure enough safety usually depends on the analogies of engineering experience. This method is convenient but the value of thickness might be over-conservative. Besides, some crucial factors also may not be considered, such as rock type, quality of rock system, etc. This method is only applicable to the preliminary estimate. Therefore, in view of those problems, some other theories and methods have been adopted by researchers, and lots of achievements are gained. PESENDORFER and LOEW [2] obtained the change rule of transient pressure from deep tunnel in fracture and karstified limestones according to experimental observations. YAN et al [3] conducted some further researches and obtained the influence of vibration. JIANG et al [4] analyzed the stability of subgrade cave roofs in karst region with catastrophe

Foundation item: Project(2013CB036004) supported by the National Basic Research Program of China; Project(51378510) supported by the National Natural Science Foundation of China
Received date: 2016−01−08; **Accepted date:** 2016−04−18
Corresponding author: YANG Xiao-li, Professor, PhD; Tel: +86−14789933669; E-mail: yangky@aliyun.com

theory and obtained the relevant function formulas. But these methods are not based on the strict stress-strain relation of geomaterials.

This work proposes a tangent method for nonlinear failure criterion, and makes deep studies in tunnel side slope and foundation. The limit analysis method has a wide range of applications in geotechnical engineering. Based on the several established models, FRALDI and GUARRACINO [5, 6] analyzed and calculated upper bound solutions of collapse press at tunnel roof and tunnel face in detail. Functional catastrophe theory is employed in this study to explain catastrophic failure, and it has unique advantages in solving complicated problems.

2 Summary of catastrophe theory

2.1 Elementary catastrophe theory

This kind of theory is put forward, and developed some researchers. The aim of catastrophe theory is to study discontinue change phenomenon in nature world. Usually, the sudden changes result from a slow, smooth, and small change under several control variables. The implicit function theorem, Morse lemma, and Thorn splitting lemma are the fundamental of catastrophe theory [7, 8].

According to the current theoretical research, there has been seven kinds of catastrophe type [9]. As is shown in Table 1, the main purpose of the analysis with catastrophe theory is to establish the total potential energy equation of the whole system. Fold and cusp catastrophe models are relatively simpler than others, and they are most widely used to determine the bearing capacity of rock-socked piles or the safety thickness of rock system. The total potential function is set up, which is closely related to the state variable and the control variable. Then, the derivative and second order derivative of potential function are acquired. Finally, the equilibrium surface and bifurcation set equations are obtained. By solving the above functions and according to relevant chart analysis, the necessary and sufficient conditions of studied system are available when instability happens.

Compared with traditional research method, engineering analogy and calculation method belong to half theoretical and semi-empirical structural mechanical analysis methods, and they are affected by many factors. But catastrophe theory can explain the discontinuous phenomena, and it considers this kind of problem from another new perspective.

2.2 Functional catastrophe theory

DU [10] suggested that functional variational theory and catastrophe theory could be linked to a certain extent, and the relevant formula had been deduced based on Thom splitting lemma. Functional catastrophe theory is considered to be an advanced catastrophe theory, and it is applied to economic field at first.

The total potential function of studied system should be expressed as a definite integral, which is

$$J[y]=\int_{x_2}^{x_1}F\left(x,f\left(x\right),f'\left(x\right)\right)\mathrm{d}x \tag{1}$$

where $f\left(x\right)\in C^3[x_1,x_2]$, and $f(x)$ is the function of detaching curve of studied system. By designating the first derivative of $J[y]$ to zero and integrating by parts, the first variation is obtained as

$$\frac{\partial F}{\partial f\left(x\right)}-\frac{\mathrm{d}}{\mathrm{d}x}\left(\frac{\partial F}{\partial f'\left(x\right)}\right)=0 \tag{2}$$

The Euler equation does not meet the variation condition of potential function. According to the functional catastrophe theory, another control condition is derived by designating the second derivation of $J[y]$ to zero and integrating by parts:

$$\frac{\partial^2 F}{\partial f\left(x\right)^2}-2\frac{\mathrm{d}}{\mathrm{d}x}\left(\frac{\partial^2 F}{\partial f\left(x\right)\partial f'\left(x\right)}\right)+\frac{\mathrm{d}^2}{\mathrm{d}x^2}\left(\frac{\partial^2 F}{\partial f'\left(x\right)^2}\right)=0 \tag{3}$$

Equations (2) and (3) are the necessary and sufficient conditions of functional catastrophe theory. The challenge is to deduce the total potential function with finite integral, and then get the function of $F\left(x,f\left(x\right),f'\left(x\right)\right)$. Functional catastrophe theory firmly

Table 1 Overview of elementary catastrophe theory

Name	Dimension of control variable	Dimension of state variable	Standard form of potential function
Fold	1	1	$x^3/3+ax$
Cusp	1	1	$x^4/4+ax^2/2+bx$
Swallowtail	3	1	$x^5/5+ax^3/3+bx^2/2+cx$
Butterfly	4	1	$x^6/6+ax^4/4+cx^2/3+bx/2+dx$
Elliptic umbilic	3	2	$x^3-xy^2+c(x^2+y^2)+ax^2+bx$
Hyperbolic umbilic	3	2	$x^3+y^3+cxy+ax^2+bx$
Parabolic umbilic	4	2	$x^4-x^2y+cx^2+dy^2+ax+by$

explains the discontinuity of system variation. The next step is to obtain the expression of $f(x)$. However, there still exist unknown values in $f(x)$, so the boundary conditions and geometric conditions of cross section could help to deduce the final analysis formula.

3 Stability analysis of tunnel floor in karst area

Karst is one of the most common tunnel hazards in tunnel engineering. According to the engineering projects and the results of ZHANG et al [11], it is known that karst caves usually lie in layered limestone areas. The system, as shown in Fig. 1, is composed by tunnel floor and karst cave roof. It has great important effects on the tunnel waterproof and load-bearing. The rock system has a certain safety thickness in tunnel engineering.

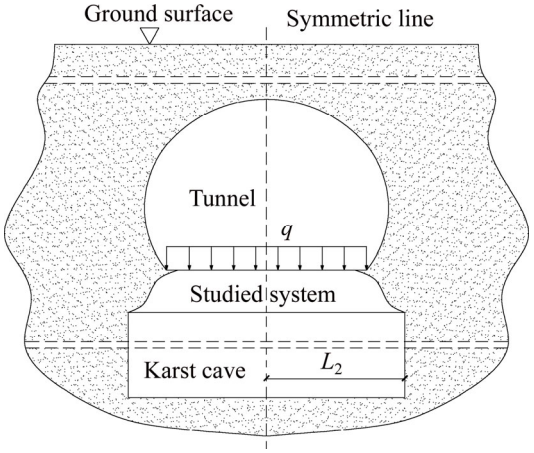

Fig. 1 Geometric boundary of tunnel with underlying cave

3.1 Upper bound theorem

CHEN [12] had introduced limit analysis method in detail which includes upper bound analysis and lower bound analysis. The upper bound theorem states that when the velocity boundary condition is satisfied, the load derived by equating the external rate of work to the rate of the energy dissipation in any kinematically admissible velocity field is greater than or equal to actual collapse load, which is written as follows:

$$\int_v D\left(\dot{\varepsilon}_{ij}\right)\mathrm{d}V \geq \int_S T_i v_i \mathrm{d}S + \int_v F_i v_i \mathrm{d}V \tag{4}$$

where $D(\dot{\varepsilon}_{ij})$ indicates the internal energy dissipation rate of plastic strain; T_i and F_i are external forces; T_i is the surcharge load on the boundary while F_i is the body force; v_i is the velocity along the velocity discontinuity surface; S and V are the surface area and the volume of studied system respectively. The studied system can remain stable when Eq. (4) is satisfied. The critical state is reached when each side of Eq. (4) is equal and it is the calculation basis of this method.

In addition, the theorem requires the following three basic assumptions: The material is perfectly plastic material, geometric deformation of failure mechanism is slight which can be ignored, and the associated flow rule is used to calculate the energy dissipation along the failure surface [13, 14].

In order to analyze the safety thickness of the studied system on the basis of the functional catastrophe theory and for the sake of simplicity, the influence of gravity is considered while the effect of tectonic stress is ignored. This treatment is keeping the same with previous research methods.

3.2 Hoek-Brown nonlinear failure criterion

Considering the nonlinear characteristics of rock materials, the nonlinear failure criterion is widely recognized by scholars, since the H-B yield criterion was proposed in 1980. Over the decades, it has been proven feasible in practical engineering and it also has been deeply investigated in different geotechnical conditions. The purpose of this work is aimed at the critical safety thickness of tunnel floor which is needed to keep stability. The karst cave usually occurs in relative stable rock layer. Hence, the H-B criterion is appropriate to analyze the studied system.

Hoek-Brown failure criterion has two forms of expression, which are represented by major and minor principal stresses, and represented by normal and shear stresses, respectively. Due to the fact that the normal stress and shear stress parameters of the element are needed for the calculation of internal energy dissipation, the Hoek-Brown failure criterion is expressed as follows:

$$\tau_{\mathrm{n}} = A\sigma_{\mathrm{ci}}\left(\frac{\sigma_{\mathrm{n}} + \sigma_{\mathrm{tm}}}{\sigma_{\mathrm{ci}}}\right)^B \tag{5}$$

where τ_{n} and σ_{n} are the normal stress and the shear stress, respectively. Parameters A and B are dimensionless material constants which could be obtained by triaxial tests. Especially when B=1.0, H-B criterion will degenerate into M-C linear yield criterion. σ_{ci} is the uniaxial compressive strength of the intact rock, and σ_{tm} is the tensile strength of the rock mass (σ_{tm}>0). The values of σ_{ci} and σ_{tm} can be determined by following formulas:

$$\begin{cases} \sigma_{\mathrm{m}} = \dfrac{\sigma_{\mathrm{ci}}}{2}\left(m_{\mathrm{b}} - \sqrt{m_{\mathrm{b}}^2 + 4s}\right)^B \\ m_{\mathrm{b}} = m_i \exp\left(\dfrac{I_{\mathrm{GS}} - 100}{28 - 14D}\right) \\ s = \exp\left(\dfrac{I_{\mathrm{GS}} - 100}{9 - 3D}\right) \end{cases} \tag{6}$$

where m_i is a parameter which can reflect the softness and hardness degree of the rock. I_{GS} is geological strength index and D is disturbance parameter of

jointed rock.

Through the upper bound analysis with the Hoek-Brown criterion, FRALDI and GUARRACINO [15] had already built several appropriate mechanical models and analyzed the shape of collapsed body both in deep tunnel and shallow tunnel. The analysis of functional catastrophe theory takes them as references. The obvious advantage is that the analytical expression of detach curve $f(x)$ could be deduced by upper limit theorem and the analytical mathematical method without assuming $f(x)$ in advance. But there is a crucial difference compared with the previous model. The velocity v is replaced by displacement u, because the target of functional catastrophe theory is total potential while upper bound theorem is at total dissipation.

3.3 Functional catastrophe analysis of studied system

As shown in Fig. 2, the geometric model of studied system is established according to analogous research model [16]. L_1 is the half collapse width in tunnel floor, L_2 is the half length of karst cave, and H is the critical safety thickness which is necessary to sustain stability. w is thickness of the plastic detaching zone when the rock system is destroyed. H-B criterion and the model show that there will form a symmetrical curve $f(x)$ when the broken occurred with displacement w. In order to simplify the calculation, half of the failure pattern is taken into consideration and a local coordinate system on detach curve $f(x)$ is established. Then, some algebraic equations can be deduced on the basis of geometrical relationship:

$$\begin{cases} \sin\theta = \dfrac{f'(x)}{\sqrt{1+f'(x)^2}} \\ \cos\theta = \dfrac{1}{\sqrt{1+f'(x)^2}} \end{cases} \tag{7}$$

The total potential includes the strain energy and the work of each force. In consideration of the geometrical perspective, the plastic potential function and corresponding normal and tangential plastic strain components are obtained as follows:

$$\begin{cases} h(\sigma_n,\tau_n) = f(\sigma_n,\tau_n) = \tau_n - A\sigma_{ci}\left(\dfrac{\sigma_n+\sigma_{tm}}{\sigma_{ci}}\right)^B \\ \varepsilon_n = \lambda\dfrac{\partial h}{\partial\sigma_n} = -\lambda AB\left(\dfrac{\sigma_n+\sigma_{tm}}{\sigma_{ci}}\right)^{B-1} = \dfrac{u}{w\sqrt{1+f'(x)^2}} \\ \gamma_n = \lambda\dfrac{\partial h}{\partial\tau_n} = \lambda = -\dfrac{uf'(x)}{w\sqrt{1+f'(x)^2}} \end{cases} \tag{8}$$

where λ is a scalar parameter which is greater than zero.

The function of normal stress at any point on the curve $f(x)$ could be deduced through eliminating λ and w:

$$\sigma_n = \sigma_{ci}\left[ABf'(x)\right]^{\frac{1}{1-B}} - \sigma_{tm} \tag{9}$$

Then, the function of strain energy on curve $f(x)$ is

$$U_i = \sigma_n\varepsilon_n + \tau_n\gamma_n = \left\{\sigma_{tm} - \sigma_{ci}\left(1-B^{-1}\right)\left[ABf'(x)\right]^{\frac{1}{1-B}}\right\}\cdot \frac{u}{\sqrt{1+f'(x)^2}} \tag{10}$$

where ρ is the density of rock system and q is the external load applied on tunnel floor. The works of gravity and external load are as follows:

$$\begin{cases} W_\rho = HL_2\rho u - u\int_{L_1}^{L_2}\rho f(x)\mathrm{d}x \\ W_q = qL_1u \end{cases} \tag{11}$$

From the above, the total potential function of studied system results

$$\begin{aligned} \xi\left(x,f(x),f'(x)\right) &= \int_{L_1}^{L_2} U_i\mathrm{d}s - W_\rho - W_q \\ &= u\int_{L_1}^{L_2}\left\{\sigma_{tm} - \sigma_{ci}\left(1-B^{-1}\right)\left[ABf'(x)\right]^{\frac{1}{1-B}} + \rho f(x)\right\}\mathrm{d}x - uHL_2\rho - uqL_1H \end{aligned} \tag{12}$$

where $\mathrm{d}s = \sqrt{1+f'(x)^2}\,\mathrm{d}x$ is the elementary length of the detaching curve $f(x)$.

According to the functional catastrophe theory, the standard form of total potential function can be obtained by ignoring the constant terms which are irrelevant to catastrophe:

$$J\left(x,f(x),f'(x)\right) = \int_{L_1}^{L_2}\left\{\sigma_{tm} - \sigma_{ci}\left(1-B^{-1}\right)\cdot \left[ABf'(x)\right]^{\frac{1}{1-B}} + \rho f(x)\right\}\mathrm{d}x \tag{13}$$

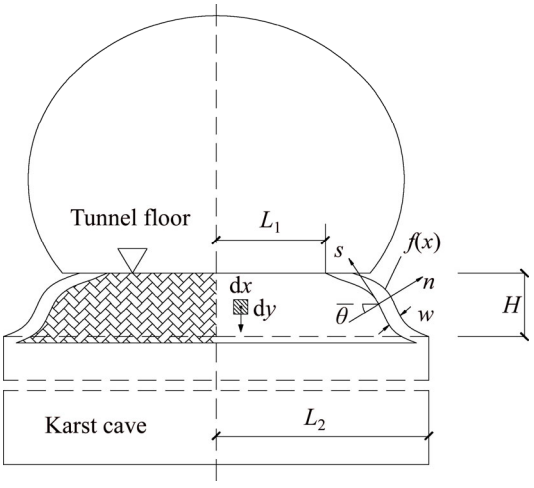

Fig. 2 Failure pattern of rock system with critical thickness

By comparing Eq. (1) and Eq. (13), the objective function which includes detaching curve $f(x)$ is obtained:

$$F\left(x, f\left(x\right), f'\left(x\right)\right) = \sigma_{\mathrm{tm}} - \sigma_{\mathrm{ci}}\left(1 - B^{-1}\right) \cdot \left[ABf'\left(x\right)\right]^{\frac{1}{1-B}} + \rho f\left(x\right) \tag{14}$$

The next critical step is to solve the explicit expression of detaching curve $f(x)$ by using boundary conditions and the critical conditions of functional catastrophe theory. Following functions can be obtained by substituting Eq. (14) into necessary and sufficient conditions (Eq. (2) and Eq. (3)):

$$\rho - \frac{\mathrm{d}}{\mathrm{d}x}\left(\sigma_{\mathrm{ci}} B^{-1}\left(AB\right)^{\frac{1}{1-B}}\left[f'\left(x\right)\right]^{\frac{B}{1-B}}\right) = 0 \tag{15}$$

$$\frac{\mathrm{d}^2}{\mathrm{d}x^2}\left(\sigma_{\mathrm{ci}}\left(\frac{1}{1-B}\right)\left(AB\right)^{\frac{1}{1-B}}\left[f'\left(x\right)\right]^{\frac{2B-1}{1-B}}\right) = 0 \tag{16}$$

Equation (15) is a linear homogeneous second-order differential equation with constant coefficients. The detaching curve $f(x)$ is obtained by integrating it:

$$f\left(x\right) = A^{-\frac{1}{B}}\left(\frac{\rho}{\sigma_{\mathrm{ci}}}\right)^{\frac{1-B}{B}}\left(x - \frac{c_1}{\rho}\right)^{\frac{1}{B}} + c_2 \tag{17}$$

where c_1 and c_2 are integration constants, which can be determined by boundary conditions. Substituting Eq. (17) into Eq. (16) yields

$$\sigma_{\mathrm{ci}} A^{\frac{1}{B}}\left(\frac{\rho}{\sigma_{\mathrm{ci}}}\right)^{\frac{2B-1}{B}}\left(2B-1\right)\left(x - \frac{c_1}{\rho}\right)^{-\frac{1}{B}} = 0 \tag{18}$$

Equation (18) is one of the second order catastrophic conditions, and it should be satisfied for any value of x. Therefore, the value of B only has to be 0.5.

In order to make sure the shape of failure rock, it is necessary to evaluate c_1 and c_2. After the tunnel excavation, the stress of tunnel floor will be redistributed. So, the shear stress should be equal to zero when x=L_1. The functions of shear stress are written as

$$\begin{cases} \tau_{xy} = \dfrac{1}{2}\sigma_{\mathrm{n}} \sin 2\theta - \tau \cos 2\theta \\ \cos 2\theta = \dfrac{f'\left(x\right)^2 - 1}{f'\left(x\right)^2 + 1},\ \sin 2\theta = \dfrac{2f'\left(x\right)}{f'\left(x\right)^2 + 1} \end{cases} \tag{19}$$

Then, the expression of c_1 is obtained by designating $\tau_{xy}(x = L_1, y = 0)$ to zero:

$$c_1 = \rho L_1 \tag{20}$$

According to the geometrical relationships illustrated in the Fig. 2, following formulas should be satisfied:

$$\begin{cases} f\left(x = L_1\right) = 0 \\ f\left(x = L_2\right) = H \end{cases} \tag{21}$$

By substituting Eq. (17) into Eq. (21), following equation is derived:

$$c_2 = 0 \tag{22}$$

$$H = A^{-2}\frac{\rho}{\sigma_{\mathrm{ci}}}\left(L_2 - L_1\right)^2 \tag{23}$$

By substituting Eq. (20), Eq. (22), and the value of B into Eq. (17), the explicit function of detaching curve $f(x)$ is obtained:

$$f\left(x\right) = A^{-2}\frac{\rho}{\sigma_{\mathrm{ci}}}\left(x - L_1\right)^2 \tag{24}$$

On the basis of upper bound theorem and the boundary condition, there are

$$\begin{cases} \xi\left(x, f\left(x\right), f'\left(x\right)\right) = 0 \\ F - f'\left(x\right)\dfrac{\partial F}{\partial f'\left(x\right)}\Big|_{x=L_2} = 0 \end{cases} \tag{25}$$

By substituting Eq. (24) into Eq. (25), there is

$$\sigma_{\mathrm{tm}}\left(L_2 - L_1\right) + \frac{2}{3}A^{-2}\frac{\rho^2}{\sigma_{\mathrm{ci}}}\left(L_2 - L_1\right)^3 - HL_2\rho - qL_1 = 0 \tag{26}$$

There are three unknowns which are more than the number of control conditions. The mutual influences can not be derived directly because of the lack of control requirement. Therefore, in this failure model, the lower boundary of collapsed block is exactly the range of karst cave. The safety thickness H and the half collapse width in tunnel floor L_1 are available by solving these two simultaneous equations Eq. (23) and Eq. (26).

When the actual thickness of rock system is thinner than H, L_1 will increase and the length of $f(x)$ will decrease. Through relevant calculation and analysis, it can be known that the work of internal energy is less than the work of external forces, in other words, the studied system cannot keep stable. On the contrary, if the requirement of Eq. (4) is satisfied when the actual thickness is greater than the theoretical value, this means that the rock system can remain stable in this failure mode. Therefore, the value of H determined by Eq. (23) and Eq. (26) is the critical thickness to sustain the system stability.

3.4 Maximum of critical thickness

The upper collapse width gradually decreases with the increase of thickness. When L_1 reaches its minimum (L_1=0), the load on tunnel floor has no effect on collapsed block, and the failure mode is shown in Fig. 3.

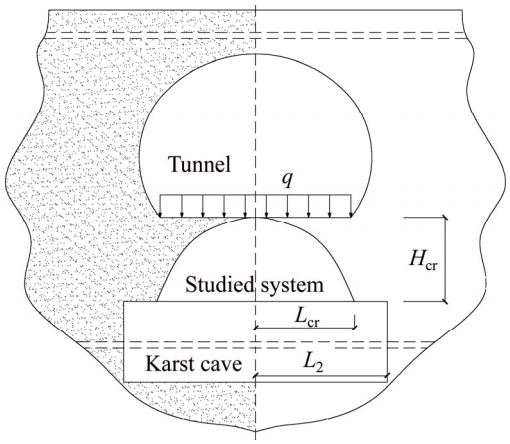

Fig. 3 Failure pattern of rock system with maximum thickness

In this case, H_{cr} is the maximum of critical thickness to keep system stable, and it is also the minimum thickness to make tunnel and karst cave independent. The number of unknowns is equal to the number of control conditions, so the lower length of collapsed block could be derived directly. The total potential function of studied system results

$$\begin{aligned}\xi\left(x,f\left(x\right),f'\left(x\right)\right)&=\int_0^{L_{cr}}U_i\mathrm{d}s-W_\rho\\&=u\int_0^{L_{cr}}\left\{\sigma_{tm}-\sigma_{ci}\left(1-B^{-1}\right)\left[ABf'\left(x\right)\right]^{\frac{1}{1-B}}+\right.\\&\left.\rho f\left(x\right)\right\}\mathrm{d}x-uH_{cr}L_{cr}\rho\end{aligned}\tag{27}$$

where L_{cr} is half lower length of collapsed block, and H_{cr} is maximum thickness of studied system. After similar analysis and calculation, it can be known that the expression of $f(x)$ remains the same. The explicit forms of H_{cr} and L_{cr} are obtained as

$$\begin{cases}L_{cr}=\dfrac{A}{\rho}\sqrt{3\sigma_{tm}\sigma_{ci}}\\H_{cr}=\dfrac{3\sigma_{tm}}{\rho}\end{cases}\tag{28}$$

When the instability occurs, the collapse region would not extend to tunnel floor under this situation. The tunnel and karst cave are uncorrelated in theory, and the tunnel floor is in a special state. The change of tunnel parameters will not affect the shape or the thickness of studied system.

Meanwhile, there is still an implicit that the half length of karst cave L_2 must be greater than or equal to L_{cr}.

4 Comparison and analysis

4.1 Value of parameter *B*

Strength function, defined by Eq. (5), is associated with Mohr envelope theory. In particular, a similar formula could be derived with using Mohr envelope. The relevant parameters have new significance. A is the scale parameter controlling the magnitude of shear strength. σ_{tm}/σ_{ci} is the shift parameter that controlling the location of the envelope on the σ axis. B is the control parameter of curvature of the envelope.

The restricted condition of B is $0<B\leq1$. But it can be drawn from the Mohr envelop that the radius curvature of τ_n is less than radius of the tangential Mohr circle [17] when $B<0.5$. Therefore, B should be greater than 0.5.

When B is equal to 1, the H-B criterion will degenerate to the linear M-C criterion. When B is equal to 0.5, this relation is exactly a generalization of Griffith's yield criterion [18], which is suitable for rock instability. That is to say, B=0.5 is one of most probable catastrophic failures combined with the consequence of functional catastrophe theory.

4.2 Shape of detaching curve *f*(*x*)

The outline of detaching zone is determined by the explicit function of detaching curve $f(x)$. It can be known from Eq. (24) that the boundary curve of detaching zone is a part of parabola. LI [19] had conducted a series experiments to study the deep tunnel collapse characteristics with a plane strain model test device, while the literatures [20−23] had researched the shape and dimensions of collapsed block in tunnel with the help of analytical approaches numerical simulations.

Although their studies are aimed at the vault of tunnel, the geological conditions and instability model are similar to those in this work. Hence, it can be used for comparison and get some illustrations. The nonlinear fitted curves of detaching zone are $y=1.224x^{1.976}$ and $y=2.15(x-0.94)^{1.93}$. According to the above results, the shape of detaching curve is an approximate parabola, which is consistent with the analytical result (i.e., Eq. (24)) in this work.

5 Discussion of analytical results

The factors discussed in this work include safety thickness H and the half collapse width of tunnel floor L_1. From the above analysis, the relationships between each parameter are available through solving simultaneous equations Eq. (23) and Eq. (26). Preliminary inference can be deduced that, based on the H-B criterion and functional catastrophe theory, the critical thickness of rock system is mainly influenced by compressive strength σ_{ci}, tensile strength σ_{tm}, the external load on tunnel floor q, the density of rock system ρ and dimensionless parameter A.

In order to investigate the effects of single parameter in karst area, several different data are set, and the values of H and L_1 are calculated. As given in the Table 2, L_2 is selected as independent variable.

Table 2 Calculating results of safety thickness under different L_2

L_2/m	σ_{ci}/MPa	σ_{tm}/MPa	ρ/(kN·m^{-3})	A	q/kPa	L_1/m	H/m
2	40	σ_{ci}/25	25	0.2	300	0.68	0.27
2.5	40	σ_{ci}/25	25	0.2	300	0.83	0.44
3	40	σ_{ci}/25	25	0.2	300	0.98	0.64
3.5	40	σ_{ci}/25	25	0.2	300	1.11	0.89
4	40	σ_{ci}/25	25	0.2	300	1.23	1.20
4.5	40	σ_{ci}/25	25	0.2	300	1.32	1.58
5	40	σ_{ci}/25	25	0.2	300	1.40	2.03
5.5	40	σ_{ci}/25	25	0.2	300	1.44	2.58
6	40	σ_{ci}/25	25	0.2	300	1.46	3.22
6.5	40	σ_{ci}/25	25	0.2	300	1.43	4.02
7	40	σ_{ci}/25	25	0.2	300	1.40	4.99

The selection of relevant parameters in Table 2 is based on experiments and engineering data. The results show that the value of safety thickness increases with the half length of cave span L_2. The functional catastrophe theory researches one of the most probable failure situations with total potential. With value of L_2 increasing, the effected width in tunnel floor extends. But it shrinks rather than keeping growing when a certain threshold is reached. And it will incline to a constant which is the most dangerous region in tunnel floor when the instability happens. Therefore, it is necessary to consolidate this area with appropriate methods in case of the catastrophic failure.

The rock stratum between tunnel and cave is detaching block. The outline of block is primarily determined by L_1, H and the shape of detaching curve. The detaching curve $f(x)$ is a part of parabola according to previous analysis. Figure 4 shows the relationship between dimensionless parameter A and half collapse width L_1. Firstly, supposing that the span of tunnel is middle (about 8 m), Fig. 4(a) simulates the situation of underlying karst cave with small span (L_2=3 m) while Fig. 4(b) simulates a cave with large span (L_2=6 m). Other values of relevant parameters are as follows: q=300 kPa, ρ=27.5 kN/m^3, σ_{tm}=σ_{ci}/20, σ_{ci}=30 MPa and σ_{ci}=50 MPa. The results indicate that the value of L_1 will increase with the increase of A. But the growth rate gradually becomes slower, and it finally approaches to a constant. The variation trends are the same with respect to the two different situations of tunnel and cave. Besides, it also can be seen from Fig. 4 that the change of L_1 affected by A is not great.

Figure 5 shows the variation of H affected by parameter σ_{ci} under different value of A, when σ_{tm}=σ_{ci}/25, q=300 kPa, ρ=25 kN/m^3 and L_2=5 m. The bigger

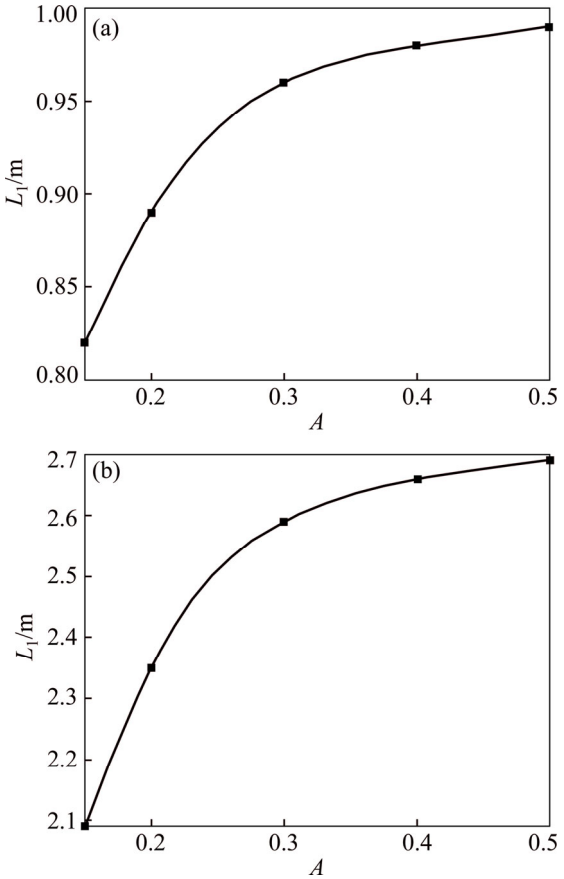

Fig. 4 Effects of parameter A on L_1: (a) L_2=3 m; (b) L_2=6 m

magnitude of σ_{ci} means the better stability of rock stratum, so the safety thickness also decreases. And A is advantageous to the stability of rock system.

Figure 6 indicates the change of L_1 influenced by σ_{ci}. Four different σ_{tm} groups are selected to analyze in detail, when A=0.2, q=300 kPa, ρ=25 kN/m^3 and L_2=5 m. It can be seen that both of them have considerable effects on L_1. The value enlarges with the increasing of σ_{tm}/σ_{ci} ratio or σ_{ci}. In other words, the rock stratum is more compact and

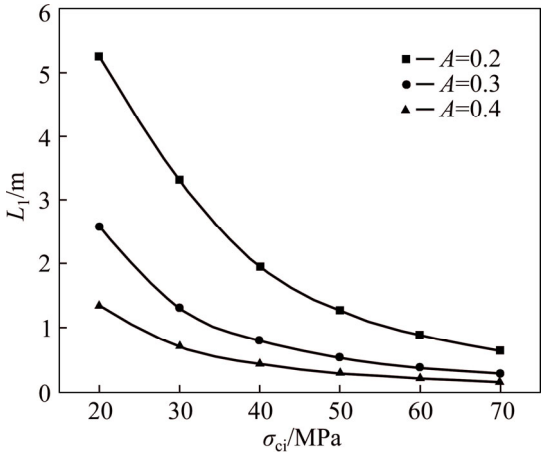

Fig. 5 Effects of parameter σ_{ci} on H

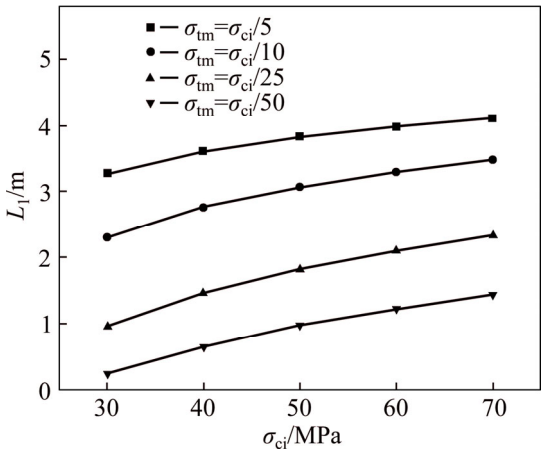

Fig. 6 Effects of parameter σ_{ci} on L_1

the detaching block will be larger, when the compressive strength and tensile strength are larger.

Figures 7 and 8 respectively illustrate the variation of H and L_1 with different values of q and ρ, when A=0.2, L_2=5 m, σ_{ci}=40 MPa and σ_{tm}=σ_{ci}/25. Similar to previous researches, external load q is not conducive to the stability of tunnel, and safety thickness H increases with q. But on the contrary, the half collapse width L_1 shrinks. As can be seen, the safety thickness H grows large with ρ,

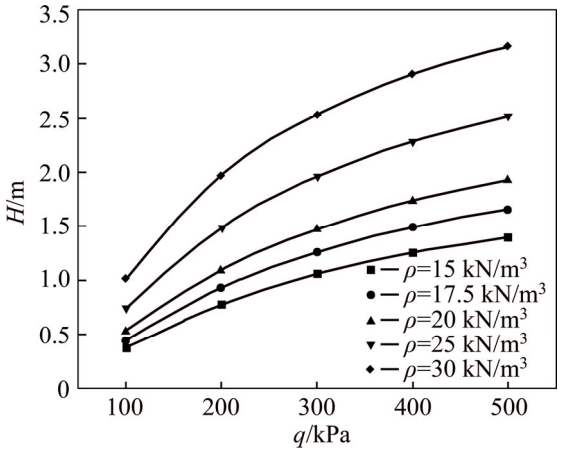

Fig. 7 Effects of parameter q on H

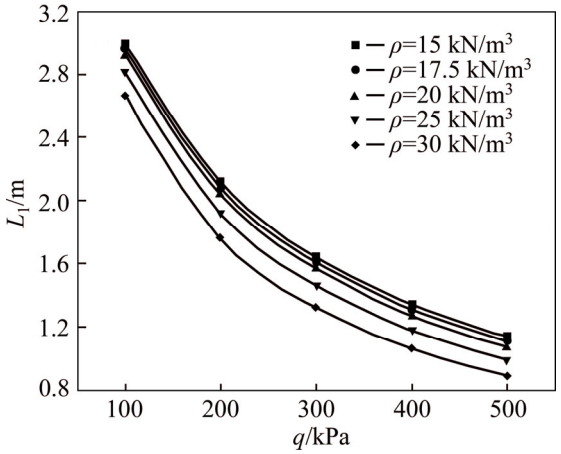

Fig. 8 Effects of parameter q on L_1

but it shows the opposite trend in L_1. Through the longitudinal observation and contrast, there is a preliminary conclusion that different values of ρ have a larger effect on H while it has less effect on L_1. In order to make certain this rule, further calculation and comparison are necessary.

Next, four groups of ρ are used for the further study of the half collapse width L_1 under different L_2. The result is shown in Fig. 9, when A=0.2, q=300 kPa, σ_{ci}= 40 MPa and σ_{tm}=σ_{ci}/25. It can be found that the change rule of L_1 along with L_2 is the same as the data in Table 2. But the magnitude of L_1 will not change with ρ when the span of karst cave is relatively small (L_2<3 m). In other situations, although the affect area gradually decreases, the total variation generally maintains within a narrow range. That is to say, ρ is not a principal factor which influences the value of half collapse width L_1.

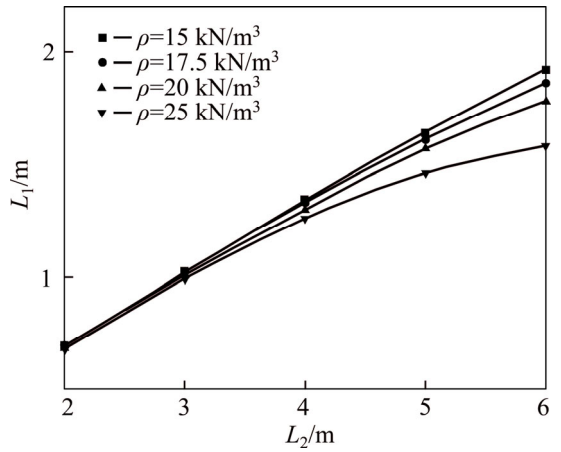

Fig. 9 Effects of parameter ρ on L_1

As illustrated in Eq. (28), the major factors influencing L_{cr} include ρ, A, σ_{tm} and σ_{ci}, while the main factors affecting H_{cr} are σ_{tm} and ρ. Both of them have very concise expressions, and the general effect of each parameter can be concluded easily without using any

chart. Table 3 is adopted to investigate the effect and trend of different parameters.

It can be seen from the Table 3 that all the relevant parameters have obvious effects on L_{cr}. Similarly, those parameters except A also have great influences on H_{cr}.

Table 3 Calculation results of L_{cr} and H_{cr}

σ_{ci}/MPa	σ_{tm}/MPa	ρ/(kN·m^{-3})	A	L_{cr}/m	H_{cr}/m
30	σ_{ci}/50	25	0.2	5.88	7.2
40	σ_{ci}/50	25	0.2	7.84	9.6
50	σ_{ci}/50	25	0.2	9.80	12
40	σ_{ci}/20	25	0.2	12.39	24
40	σ_{ci}/60	25	0.2	7.16	8
40	σ_{ci}/100	25	0.2	5.54	4.8
40	σ_{ci}/50	25	0.1	3.92	9.6
40	σ_{ci}/50	25	0.3	11.76	9.6
40	σ_{ci}/50	25	0.5	19.60	9.6
40	σ_{ci}/50	17.5	0.2	11.20	13.71
40	σ_{ci}/50	22.5	0.2	8.71	10.67
40	σ_{ci}/50	27.5	0.2	7.13	8.72

6 Conclusions

1) According to the upper bound theorem, the outline of detaching block of tunnel floor with underlying cave is presumed. Then the total potential function of studied system is established based on the Hoek-Brown criterion. The explicit expressions of equations which determine the safety thickness H and detaching curve $f(x)$ are obtained on the basis of the functional catastrophe theory and boundary conditions. The maximum safety thickness H_{cr} is obtained under the assumptions that tunnel and karst cave are independent, and the actual half length of cave L_2 is greater than the theoretical solution L_{cr}.

2) The shape of detaching block is bounded by safety thickness H, L_2, half collapse width L_1 and detaching curve $f(x)$. The results are compared with experiment and numerical simulation, and it is convinced that the shape of $f(x)$ is a part of parabola.

3) The principal factors influencing H and L_1 are as follows: compressive strength σ_{ci}, tensile strength σ_{tm}, external load on tunnel floor q, the density of rock ρ and dimensionless parameter A. Further calculation and analysis are adopted in order to study the influence of single variable. The results show that σ_{ci}, σ_{tm} and A are conducive to the stability of rock system while q and ρ have opposite effects instead. The value of half collapse width L_1 increases with L_2, A, σ_{ci} and σ_{tm}. But the influence range of A is quite smaller than others. The value of L_1 shows a trend of decrease with the increase in ρ. It has not obvious change when the span of cave is relatively small.

References

[1] GUGLIELMETTI V, GRASSO P, MAHTAB A, XU S. Mechanised tunnelling in urban areas [J]. Tunnels and Tunnelling International, 2007, 12: 21−23.

[2] PESENDORFER M, LOEW S. Subsurface exploration and transient pressure testing from a deep tunnel in fractured and karstified limestones [J]. International Journal of Rock Mechanics and Mining Sciences, 2010, 47(1): 121−137.

[3] YAN C B, XU G Y, ZUO Y J. Destabilization analysis of overlapping underground chambers induced by blasting vibration with catastrophe theory [J]. Transactions of Nonferrous Metals Society of China, 2006, 16(3): 735−740.

[4] JIANG C, ZHAO M H, CAO W G. Stability analysis of subgrade cave roofs in karst region [J]. Journal of Central South University of Technology, 2008, 15(2): 38−44.

[5] FRALDI M, GUARRACINO F. Limit analysis of collapse mechanisms in cavities and tunnels according to the Hoek–Brown failure criterion [J]. International Journal of Rock Mechanics and Mining Sciences, 2009, 46(4): 665−673.

[6] FRALDI M, GUARRACINO F. Analytical solutions for collapse mechanisms in tunnels with arbitrary cross sections [J]. International Journal of Solids and Structures, 2010, 47(2): 216−223.

[7] YANG X L, DU D C. Upper bound analysis for bearing capacity of nonhomogeneous and anisotropic clay foundation [J]. KSCE Journal of Civil Engineering, 2016, 20(7): 2702−2710.

[8] YANG Xiao-li, XIAO Hai-bo. Safety thickness analysis of tunnel floor in karst region based on catastrophe theory [J]. Journal of Central South University, 2016, 23(9): 2364−2372.

[9] YANG X L, LI W T. Reliability analysis of shallow tunnel with surface settlement [J]. Geomechanics and Engineering, 2017, 12(2): 313−326.

[10] DU X F. Functional catastrophe theory and its application in physical analytical mechanics and economical analytical mechanics [M]. The Progress of Interdisciplinary Research For Mathematics, Mechanics, Physics and High New Technology, 2002: 35−45. (in Chinese)

[11] ZHANG C P, HAN K H, FANG Q, ZHANG D L. Functional catastrophe analysis of collapse mechanisms for deep tunnels based on the Hoek–Brown failure criterion [J]. Journal of Zhejiang University, 2015, 15(9): 723−731.

[12] CHEN W F. Limit analysis and soil plasticity [M]. The Netherland: Elsevier, 2013: 47−99.

[13] YANG X L, LI K F. Roof collapse of shallow tunnel in layered Hoek-Brown rock media [J]. Geomechanics and Engineering, 2016, 11(6): 867−877.

[14] LI Y X, YANG X L. Stability analysis of crack slope considering nonlinearity and water pressure [J]. KSCE Journal of Civil Engineering, 2016, 20(6): 2289−2296.

[15] FRALDI M, GUARRACINO F. Evaluation of impending collapse in circular tunnels by analytical and numerical approaches [J]. Tunnelling & Underground Space Technology, 2011, 26(4): 507−516.

[16] YANG Xiao-li, YAO Cong, ZHANG Jia-hua. Safe retaining pressures for pressurized tunnel face using nonlinear failure criterion and reliability theory [J]. Journal of Central South University, 2016, 23(3): 708−720.

[17] YANG X L, YAO C. Axisymmetric failure mechanism of a deep

cavity in layered soils subjected to pore pressure [J]. International Journal of Geomechanics, 2017: 04017031. DOI: 10.1061/(ASCE)GM.1943-5622.0000911.

[18] YANG X L, XU J S. Three-dimensional stability of two-stage slope in inhomogeneous soils [J]. International Journal of Geomechanics, 2017: 06016045. DOI: 10.1061/(ASCE)GM.1943- 5622.0000867.

[19] LI H. Instability mode and corresponding evolution law of the ground with voids induced by shallow tunneling [D]. Beijing Jiaotong University, 2013. (in Chinese)

[20] YANG X L. Effect of pore water pressure on 3D stability of rock slope [J]. International Journal of Geomechanics, 2017, DOI: 10.1061/(ASCE)GM.1943-5622.0000969.

[21] YANG X L, PAN Q J. Three dimensional seismic and static stability of rock slopes [J]. Geomechanics and Engineering, 2015, 8(1): 97−111.

[22] YANG X L, YAN R M. Collapse mechanism for deep tunnel subjected to seepage force in layered soils [J]. Geomechanics and Engineering, 2015, 8(5): 741−756.

[23] ZHANG C P, HAN K H. Collapsed shape of shallow unlined tunnels based on functional catastrophe theory [J]. Mathematical Problems in Engineering, 2015, 2015: 1−13.

(Edited by YANG Bing)

Cite this article as: YANG Xiao-li, LI Zheng-wei, LIU Zheng-an, XIAO Hai-bo. Collapse analysis of tunnel floor in karst area based on Hoek-Brown rock media [J]. Journal of Central South University, 2017, 24(4): 957−966. DOI: 10.1007/s11771-017-3498-5.